Electromagnetic properties of the neutrinos in γp collision at the LHC

İ. Şahin[*]

Department of Physics, Zonguldak Karaelmas University, 67100 Zonguldak, Turkey
(Received 13 November 2011; published 6 February 2012)

We have investigated nonstandard $\nu\bar{\nu}\gamma$ and $\nu\bar{\nu}\gamma\gamma$ couplings via $\nu\bar{\nu}$ production in a γp collision at the LHC. We obtain 95% confidence level bounds on $\nu\bar{\nu}\gamma$ and $\nu\bar{\nu}\gamma\gamma$ couplings by considering three different forward detector acceptances: $0.0015 < \xi < 0.15$, $0.0015 < \xi < 0.5$, and $0.1 < \xi < 0.5$. We show that the reaction $pp \rightarrow p\gamma p \rightarrow p\nu\bar{\nu}qX$ provides more than eight orders of magnitude improvement in neutrino-two photon couplings compared to LEP limits.

I. INTRODUCTION

Neutrinos play an important role in the evolution of the Universe and in many astrophysical processes. Their properties are under intense study and some rigorous restrictions have been obtained on their anomalous properties from controlled experiments and astrophysical observations. The Large Hadron Collider (LHC) offers the opportunity of a very rich physics program. It is remarkable to examine the potential of LHC for probing anomalous neutrino properties.

In the minimal extension of the standard model (SM) with massive neutrinos, radiative corrections induce tiny couplings of $\nu\bar{\nu}\gamma$ and $\nu\bar{\nu}\gamma\gamma$ [1–5]. Despite the fact that minimal extension of the SM induces very small couplings, there are several models beyond the SM predicting relatively large $\nu\bar{\nu}\gamma$ and $\nu\bar{\nu}\gamma\gamma$ couplings. Therefore it is meaningful to search for electromagnetic properties of the neutrinos in a model-independent way. Electromagnetic properties of the neutrinos have important implications on particle physics, astrophysics, and cosmology. Probing electromagnetic structure of the neutrinos is important for understanding the physics beyond the SM and contributes to the studies in astrophysics and cosmology.

ATLAS and CMS collaborations have a program of forward physics with extra detectors located at distances of 220 m and 420 m from the interaction point [6–8]. The physics program of this new instrumentation covers soft and hard diffraction, high energy photon-induced interactions, low-x dynamics with forward jet studies, large rapidity gaps between forward jets, and luminosity monitoring [9–27]. The forward detector equipment allows us to detect intact scattered protons with some momentum fraction loss $\xi = (|\vec{p}| - |\vec{p}'|)/|\vec{p}|$. Here $\vec{p}$ is the momentum of incoming proton and $\vec{p}'$ is the momentum of intact scattered proton. Complementary to proton-proton interactions, forward detector equipment at the LHC allows us to study photon-photon and photon-proton interactions at energies higher than at any existing collider. Photon-induced reactions in a hadron-hadron collision were

observed in the measurements of CDF collaboration [28–31]. The reactions such as $p\bar{p} \rightarrow p\gamma\gamma\bar{p} \rightarrow pe^+e^-\bar{p}$ [28,31], $p\bar{p} \rightarrow p\gamma\gamma\bar{p} \rightarrow p\mu^+\mu^-\bar{p}$ [30,31], $p\bar{p} \rightarrow p\gamma\bar{p} \rightarrow pJ/\psi(\psi(2S))\bar{p}$ [30] were verified experimentally. These results raise interest on the potential of LHC as a photon-photon and photon-proton collider.

In this paper we have investigated anomalous $\nu\bar{\nu}\gamma$ and $\nu\bar{\nu}\gamma\gamma$ couplings via $\nu\bar{\nu}$ production in a γp collision at the LHC. A quasireal photon emitted from one proton beam can interact with the other proton and produce a $\nu\bar{\nu}$ pair through deep inelastic scattering. Emitted quasireal photons are described by equivalent photon approximation (EPA) [26,32,33]. Their virtuality is very low and it is a good approximation to assume that they are on-mass-shell. In Fig. 1 we show a schematic diagram for our main reaction $pp \rightarrow p\gamma p \rightarrow p\nu\bar{\nu}qX$. Intact scattered protons after the collision can be detected by the forward detectors. In correlation with central detectors a distinctive signal for the γp collision can be identified. In particular, two experimental signatures arise for any reaction in a γp collision [27]: In the framework of EPA, emitted quasireal photons from the protons have a low virtuality and scattered with small angles from the beam pipe. Therefore when a proton emits a quasireal photon it should also be scattered with a small angle. Hence, intact scattered protons exit the central detector without being detected. This causes a decrease in the energy deposit in the corresponding forward region compared to the case in which the proton remnants are detected by the calorimeters. Consequently, for a γp collision, one of the forward regions of the central detector has a significant lack of energy. The region with a lack of particles defines a forward large-rapidity gap. Usual pp deep inelastic processes can be rejected by applying a selection cut on this quantity. Another experimental signature is provided by the forward detectors. When an intact proton is scattered with a large pseudorapidity it escapes detection from the central detectors. But since its energy is lower than the beam energy, its trajectory decouples from the beam path into the very forward region. Forward detectors can detect particles with a large pseudorapidity. The detection of intact protons by the forward detectors provides a characteristic signature. The detection of the $pp \rightarrow p\gamma p \rightarrow p\nu\bar{\nu}qX$
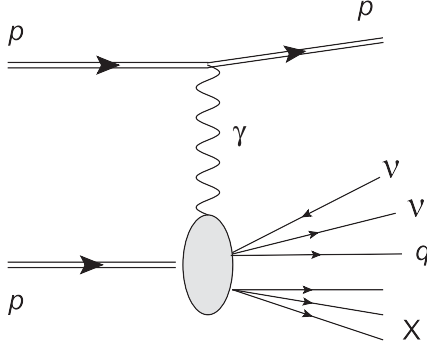
*inancsahin@karaelmas.edu.tr

FIG. 1. Schematic diagram for the reaction $pp \rightarrow p\gamma p \rightarrow p\nu\bar{\nu}qX$.

reaction involves in addition to the above signatures, a missing energy signature due to $\nu\bar{\nu}$ production. The missing energy signature due to neutrinos has a different characteristic compared to the case of missing protons. First, a missing energy signature due to neutrinos is not only observed in the forward regions of the central detector but also in central regions of it. Second, in the case of missing protons there should be a missing charge equivalent to the charge of proton. Third, the most important difference is that protons scattered with small angles are not genuinely missing. Forward detectors can detect them. On the other hand, this is not the case for neutrinos.

Forward detectors have a capability to detect intact scattered protons with momentum fraction loss in the interval $\xi_{\min} < \xi < \xi_{\max}$. The interval $\xi_{\min} < \xi < \xi_{\max}$ is called the acceptance of the forward detectors. The acceptance of $0.0015 < \xi < 0.15$ is proposed by the ATLAS Forward Physics (AFP) Collaboration [6,7]. On the other hand, the CMS-TOTEM forward detector scenario proposes an acceptance of $0.0015 < \xi < 0.5$ [8]. Since the forward detectors can detect protons in a continuous range of ξ one can impose some cuts and choose to work in a subinterval of the whole acceptance region. In this paper we consider three different forward detector acceptances; $0.0015 < \xi < 0.15$, $0.0015 < \xi < 0.5$, and $0.1 < \xi < 0.5$.

New physics probes in photon-induced reactions at the LHC have been discussed in the literature [19–21,34–43]. It was shown in Ref. [43] that $\gamma\gamma$ collision at the LHC has a great potential to probe $\nu\bar{\nu}\gamma\gamma$ couplings. It provides more than seven orders of magnitude improvement in $\nu\bar{\nu}\gamma\gamma$ couplings compared to LEP limits [43].

II. EFFECTIVE LAGRANGIAN AND CROSS SECTIONS

We employ the following effective Lagrangian for non-standard $\nu\bar{\nu}\gamma$ coupling [44–47]

$$\mathcal{L} = \tfrac{1}{2}\mu_{ij}\bar{\nu}_i\sigma_{\mu\nu}\nu_j F^{\mu\nu}, \quad (1)$$

where μ_{ii} is the magnetic moment of ν_i and μ_{ij} $(i \neq j)$ is the transition magnetic moment. In the above effective

Lagrangian new physics energy scale Λ is absorbed in the definition of μ_{ij}. Nonstandard $\nu\bar{\nu}\gamma\gamma$ coupling can be described by the following dimension-7 effective Lagrangian [5,47–51]:

$$\mathcal{L} = \frac{1}{4\Lambda^3}\bar{\nu}_i(\alpha_{R1}^{ij}P_R + \alpha_{L1}^{ij}P_L)\nu_j\tilde{F}_{\mu\nu}F^{\mu\nu}$$
$$+ \frac{1}{4\Lambda^3}\bar{\nu}_i(\alpha_{R2}^{ij}P_R + \alpha_{L2}^{ij}P_L)\nu_j F_{\mu\nu}F^{\mu\nu}, \quad (2)$$

where $P_{L(R)} = \tfrac{1}{2}(1 \mp \gamma_5)$, $\tilde{F}_{\mu\nu} = \tfrac{1}{2}\epsilon_{\mu\nu\alpha\beta}F^{\alpha\beta}$, α_{Lk}^{ij} and α_{Rk}^{ij} are dimensionless coupling constants. We will consider the Dirac neutrino case and obtain model independent bounds on couplings in the effective Lagrangians (1) and (2).

We have rigorous experimental bounds on neutrino magnetic moment obtained from neutrino-electron scattering experiments with reactor neutrinos. These are at the order of $10^{-11}\mu_B$ [52–55]. Bounds derived from solar neutrinos are at the same order of magnitude [56]. On the other hand, we have more restrictive bounds obtained from astrophysical observations. For instance, bounds derived from energy loss of astrophysical objects give about an order of magnitude more restrictive bounds than reactor and solar neutrino probes [57–63]. Although there is a great amount of work on $\nu\bar{\nu}\gamma$ coupling, $\nu\bar{\nu}\gamma\gamma$ coupling has been much less studied in the literature. Current experimental bounds on this coupling are obtained from rare decay $Z \rightarrow \nu\bar{\nu}\gamma\gamma$ [47] and the analysis of $\nu_\mu N \rightarrow \nu_s N$ conversion [51]. The following upper bound has been obtained from the LEP data on $Z \rightarrow \nu\bar{\nu}\gamma\gamma$ decay [47]

$$\left[\frac{1\text{ GeV}}{\Lambda}\right]^6\sum_{i,j,k}(|\alpha_{Rk}^{ij}|^2 + |\alpha_{Lk}^{ij}|^2) \leq 2.85 \times 10^{-9}. \quad (3)$$

The analysis of the process $\nu_\mu N \rightarrow \nu_s N$ conversion via the Primakoff effect in the external Coulomb field of the nucleus N yields about two orders of magnitude more restrictive bound than $Z \rightarrow \nu\bar{\nu}\gamma\gamma$ decay [51].

We consider the following subprocesses of our main reaction $pp \rightarrow p\gamma p \rightarrow p\nu\bar{\nu}qX$:

(i) $\gamma u \rightarrow \nu\bar{\nu}u$ (ii) $\gamma d \rightarrow \nu\bar{\nu}d$ (iii) $\gamma c \rightarrow \nu\bar{\nu}c$

(iv) $\gamma s \rightarrow \nu\bar{\nu}s$ (v) $\gamma b \rightarrow \nu\bar{\nu}b$ (vi) $\gamma\bar{u} \rightarrow \nu\bar{\nu}\bar{u}$

(vii) $\gamma\bar{d} \rightarrow \nu\bar{\nu}\bar{d}$ (viii) $\gamma\bar{c} \rightarrow \nu\bar{\nu}\bar{c}$ (ix) $\gamma\bar{s} \rightarrow \nu\bar{\nu}\bar{s}$ (4)

(x) $\gamma\bar{b} \rightarrow \nu\bar{\nu}\bar{b}$.

In the presence of the effective interaction (1) each of the subprocesses is described by eight tree-level diagrams (Fig. 2). As we see from Fig. 2, six diagram contains nonstandard $\nu\bar{\nu}\gamma$ interactions. The analytical expression for the polarization summed amplitude square is quite lengthy so we do not present it here. But it can be written in the following form:
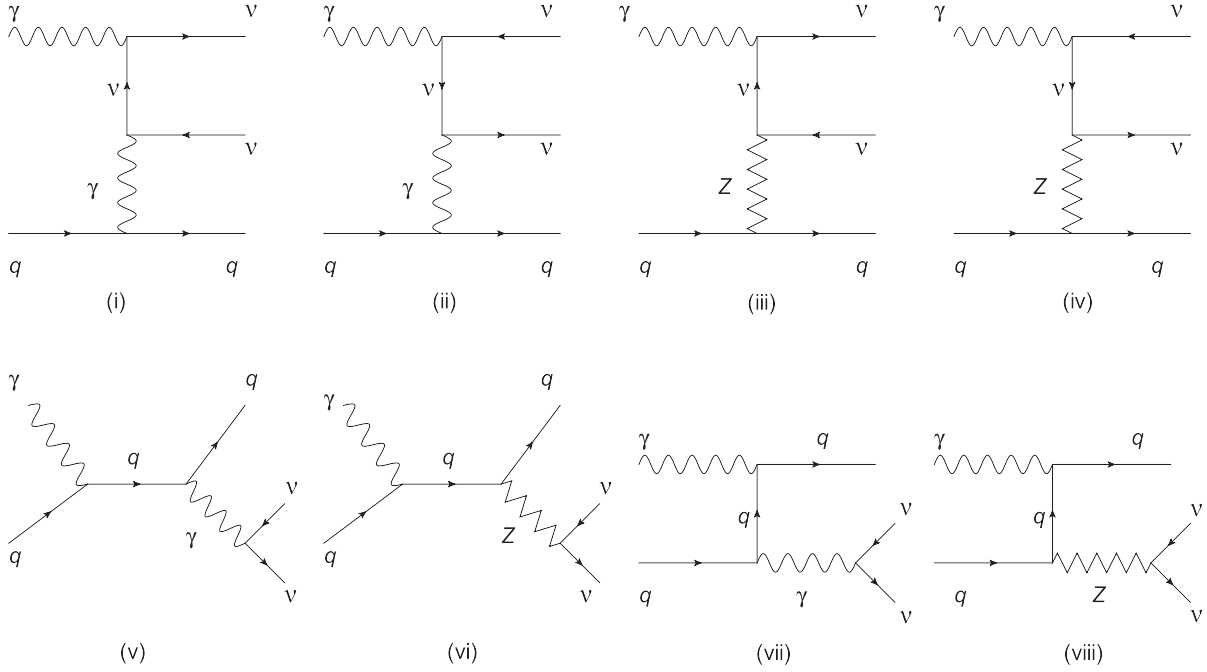
FIG. 2.   Tree-level Feynman diagrams for the subprocess $\gamma q \to \nu \bar{\nu} q$ ($q = u, d, c, s, b, \bar{u}, \bar{d}, \bar{c}, \bar{s}, \bar{b}$) in the presence of nonstandard $\nu \bar{\nu} \gamma$ coupling.

$$\sum_{i,j} \langle |M|^2 \rangle = \left(\sum_{i,j,m,n} \mu_{im} \mu_{mj} \mu_{in} \mu_{nj} \right) F_1 + \left(\sum_{i,j} \mu_{ij}^2 \right) F_2$$

$$+ \left(\sum_{i,m} \mu_{im} \mu_{mi} \right) F_3 + F_4, \qquad (5)$$

where

$$F_1 = |M_1|^2 + |M_2|^2 + M_1^\dagger M_2 + M_2^\dagger M_1$$

$$F_2 = |M_3|^2 + |M_4|^2 + |M_5|^2 + |M_7|^2 + M_3^\dagger M_5 + M_5^\dagger M_3$$

$$\qquad + M_3^\dagger M_7 + M_7^\dagger M_3 + M_4^\dagger M_5 + M_5^\dagger M_4 + M_4^\dagger M_7$$

$$\qquad + M_7^\dagger M_4 + M_5^\dagger M_7 + M_7^\dagger M_5$$

$$F_3 = M_1^\dagger M_6 + M_6^\dagger M_1 + M_1^\dagger M_8 + M_8^\dagger M_1 + M_2^\dagger M_6$$

$$\qquad + M_6^\dagger M_2 + M_2^\dagger M_8 + M_8^\dagger M_2$$

$$F_4 = 3(|M_6|^2 + |M_8|^2 + M_6^\dagger M_8 + M_8^\dagger M_6).$$

Here, $M_i (i = 1, \ldots, 8)$ are the "flavor independent" amplitudes of the diagrams shown in Fig. 2. By using a phrase "flavor independent" we mean the part of the amplitude which does not contain the coupling constants μ_{ij} or equivalently amplitude with $\mu_{ij} = 1$. Since the structure of the effective Lagrangian (1) is the same for each neutrino flavor and we omit the mass of neutrinos, M_i amplitudes are independent of the neutrino flavor. In the definitions of F_i functions, average over initial spins and sum over final spins is implied. Since it is impossible to discern final neutrino flavor, in Eq. (5) we perform a sum over flavor indices i and j.

In the case of effective interaction (2) we have three tree-level diagrams (Fig. 3). The polarization summed amplitude square can be written in the form:

$$\sum_{i,j} \langle |M|^2 \rangle = (\alpha_1^2 + \alpha_2^2) G_1 + G_2, \qquad (6)$$

where

$$\alpha_1^2 = \sum_{i,j} [|\alpha_{R1}^{ij}|^2 + |\alpha_{L1}^{ij}|^2], \quad \alpha_2^2 = \sum_{i,j} [|\alpha_{R2}^{ij}|^2 + |\alpha_{L2}^{ij}|^2] \quad (7)$$

and G_1, G_2 are some functions of the momenta. Again a sum over indices i and j has been performed. Analytical expressions for G_1 and G_2 are given in the Appendix.

In the framework of EPA, equivalent photon spectrum of virtuality Q^2 and energy E_γ is given by the following formula [26,32,33]:

$$\frac{dN_\gamma}{dE_\gamma dQ^2} = \frac{\alpha}{\pi} \frac{1}{E_\gamma Q^2} \left[\left(1 - \frac{E_\gamma}{E} \right) \left(1 - \frac{Q_{\min}^2}{Q^2} \right) F_E + \frac{E_\gamma^2}{2E^2} F_M \right],$$

$$(8)$$

where

$$Q_{\min}^2 = \frac{m_p^2 E_\gamma^2}{E(E - E_\gamma)}, \qquad F_E = \frac{4m_p^2 G_E^2 + Q^2 G_M^2}{4m_p^2 + Q^2} \quad (9)$$

$$G_E^2 = \frac{G_M^2}{\mu_p^2} = \left(1 + \frac{Q^2}{Q_0^2} \right)^{-4}, \quad F_M = G_M^2, \quad Q_0^2 = 0.71 \, \text{GeV}^2.$$

$$(10)$$

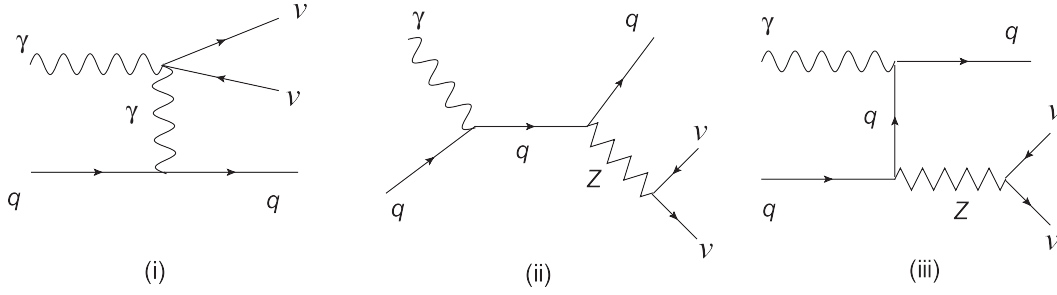Here, E is the energy of the incoming proton beam and m_p is the mass of the proton. The magnetic moment of the

FIG. 3. Tree-level Feynman diagrams for the subprocess $\gamma q \to \nu \bar{\nu} q$ ($q = u, d, c, s, b, \bar{u}, \bar{d}, \bar{c}, \bar{s}, \bar{b}$) in the presence of nonstandard $\nu \bar{\nu} \gamma \gamma$ coupling.

proton is $\mu_p^2 = 7.78$. F_E and F_M are functions of the electric and magnetic form factors. In the above EPA formula, electromagnetic form factors of the proton have been taken into consideration. After integration over Q^2 in the interval $Q_{min}^2 - Q_{max}^2$, equivalent photon spectrum can be written as [19]

$$\frac{dN_\gamma}{dE_\gamma} = \frac{\alpha}{\pi E_\gamma} \left(1 - \frac{E_\gamma}{E}\right) \left[\varphi\left(\frac{Q_{max}^2}{Q_0^2}\right) - \varphi\left(\frac{Q_{min}^2}{Q_0^2}\right)\right], \quad (11)$$

where the function φ is defined by

$$\varphi(x) = (1 + ay) \left[-\ln\left(1 + \frac{1}{x}\right) + \sum_{k=1}^{3} \frac{1}{k(1+x)^k}\right] + \frac{y(1-b)}{4x(1+x)^3}$$

$$+ c\left(1 + \frac{y}{4}\right) \left[\ln\left(\frac{1-b+x}{1+x}\right) + \sum_{k=1}^{3} \frac{b^k}{k(1+x)^k}\right], \quad (12)$$

where

$$y = \frac{E_\gamma^2}{E(E - E_\gamma)}, \qquad a = \frac{1 + \mu_p^2}{4} + \frac{4m_p^2}{Q_0^2} \approx 7.16$$

$$b = 1 - \frac{4m_p^2}{Q_0^2} \approx -3.96, \qquad c = \frac{\mu_p^2 - 1}{b^4} \approx 0.028. \quad (13)$$

The contribution to the integral above $Q_{max}^2 \approx 2$ GeV^2 is negligible. Therefore during calculations we set $Q_{max}^2 \approx 2$ GeV^2.

The cross section for the complete process $pp \to p\gamma p \to p\nu\bar{\nu}qX$ can be obtained by integrating the cross section for the subprocess $\gamma q \to \nu\bar{\nu}q$ over the photon and quark spectra:

$$\sigma(pp \to p\gamma p \to p\nu\bar{\nu}qX)$$

$$= \int_{x_{1min}}^{x_{1max}} dx_1 \int_0^1 dx_2 \left(\frac{dN_\gamma}{dx_1}\right)\left(\frac{dN_q}{dx_2}\right) \hat{\sigma}_{\gamma q \to \nu\bar{\nu}q}(\hat{s}) \quad (14)$$

Here, $x_1 = \frac{E_\gamma}{E}$ and x_2 is the momentum fraction of the proton's momentum carried by the quark. At high energies greater than proton mass it is a good approximation to write $\xi = \frac{E_\gamma}{E}$. Therefore upper and lower limits of the

dx_1 integral are $x_{1max} = \xi_{max}$ and $x_{1min} = \xi_{min}$. $\frac{dN_q}{dx_2}$ is the quark distribution function of the proton. The virtuality of the quark is taken to be $Q'^2 = m_Z^2$ during calculations. In our calculations parton distribution functions of Martin, Stirling, Thorne, and Watt [64] have been used. We always sum all the contributions from subprocesses given in Eq. (4).

Assuming only one of the matrix elements μ_{ij} is different from zero, say μ, we plot the integrated total cross section of the process $pp \to p\gamma p \to p\nu\bar{\nu}qX$ as a function of anomalous coupling μ in Fig. 4. We see from Fig. 4 that cross sections for the acceptances $0.0015 < \xi < 0.15$ and $0.0015 < \xi < 0.5$ are close to each other. On the other hand, the cross section for $0.1 < \xi < 0.5$ is considerably smaller than the others. In Fig. 5 we plot the integrated total cross section of the process $pp \to p\gamma p \to p\nu\bar{\nu}qX$ as a function of anomalous coupling α_1 for the acceptances $0.0015 < \xi < 0.15$, $0.0015 < \xi < 0.5$, and $0.1 < \xi < 0.5$. Cross sections in Fig. 5 reflect similar behavior to Fig. 4. In all results presented in this paper we assume that center-of-mass energy of the proton-proton system is $\sqrt{s} = 14$ TeV.

FIG. 4. The integrated total cross section of the process $pp \to p\gamma p \to p\nu\bar{\nu}qX$ as a function of anomalous coupling μ for three different forward detector acceptances stated in the figure. The center-of-mass energy of the proton-proton system is taken to be $\sqrt{s} = 14$ TeV.
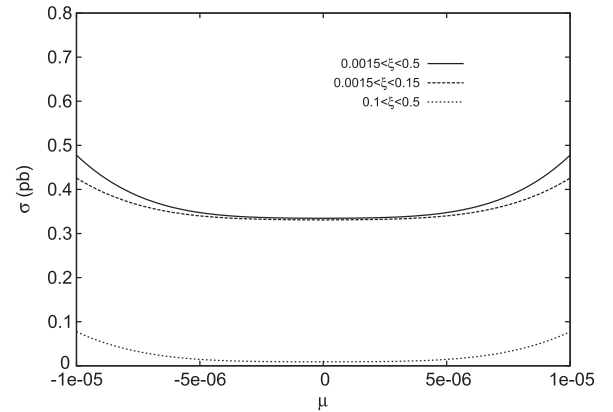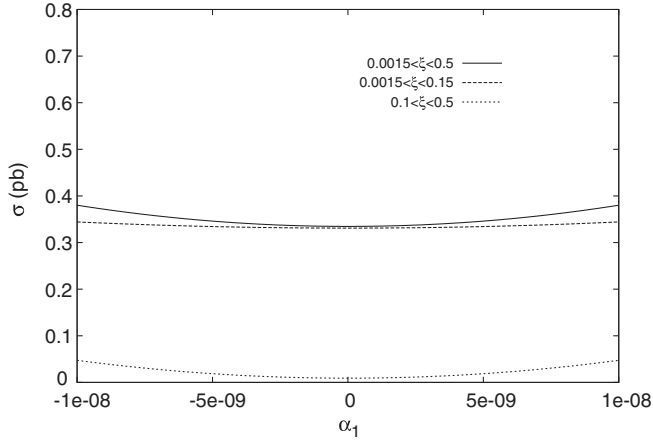
FIG. 5.   The integrated total cross section of the process $pp \rightarrow p\gamma p \rightarrow p\nu\bar{\nu}qX$ as a function of anomalous coupling α_1 for three different forward detector acceptances stated in the figure. The center-of-mass energy of the proton-proton system is taken to be $\sqrt{s} = 14$ TeV.

III. SENSITIVITY TO ANOMALOUS COUPLINGS

We have estimated 95% confidence level (C.L.) bounds using one-parameter χ^2 test without a systematic error. The χ^2 function is given by

$$\chi^2 = \left(\frac{\sigma_{\mathrm{SM}} - \sigma_{AN}}{\sigma_{\mathrm{SM}} \delta} \right)^2, \qquad (15)$$

where σ_{AN} is the cross section containing new physics effects and $\delta = \frac{1}{\sqrt{N}}$ is the statistical error. The number of

events is given by $N = \sigma_{\mathrm{SM}} L_{\mathrm{int}}$, where L_{int} is the integrated luminosity. ATLAS and CMS have central detectors with a pseudorapidity coverage $|\eta| < 2.5$. Therefore we place a cut of $|\eta| < 2.5$ for final quarks from subprocess $\gamma q \rightarrow \nu\bar{\nu}q$.

We observe from Eq. (5) that cross section including $\nu\bar{\nu}\gamma$ coupling depends on the couplings of the form; $\sum_{i,j,m,n} \mu_{im}\mu_{mj}\mu_{in}\mu_{nj}$, $\sum_{i,j} \mu_{ij}^2$, and $\sum_{i,m} \mu_{im}\mu_{mi}$. It receives contributions from all of the matrix elements μ_{kl}, $(k, l = 1, 2, 3)$. As we have mentioned in the previous section, some of the matrix elements are strictly constrained by the experiments. As far as we know the least constrained element is $\mu_{\tau\tau}$. The bound on this element is $3.9 \times 10^{-7} \mu_B$ [65]. This bound is at least 3 orders of magnitude weaker than the bounds on other matrix elements [66]. Therefore in the numerical calculations we can neglect these strictly constrained elements and assume that only $\mu_{\tau\tau}$ is nonvanishing. In Tables I, II, and III we show 95% C.L. upper bounds of the couplings $\mu_{\tau\tau}$, α_1^2 and α_2^2 for three different forward detector acceptances. We see from these tables that our limits on $\mu_{\tau\tau}$ are worse than the current experimental limit. Our most sensitive limit is approximately 5 times weaker than the DONUT bound [65]. On the other hand, we see from the tables that our bounds on α_1^2 and α_2^2 are approximately at the order of 10^{-17}–10^{-18}. It is more than 8 orders of magnitude more restrictive than the LEP bound. Forward detector acceptance of $0.1 < \xi < 0.5$ provides more restrictive bounds on both $\mu_{\tau\tau}$, α_1^2, and α_2^2 couplings with respect to the $0.0015 < \xi < 0.15$ and $0.0015 < \xi < 0.5$ cases. This

TABLE I.   95% C.L. upper bounds of the couplings $\mu_{\tau\tau}$, α_1^2, and α_2^2 for the process $pp \rightarrow p\gamma p \rightarrow p\nu\bar{\nu}qX$. We consider various values of the integrated LHC luminosities. Forward detector acceptance is $0.0015 < \xi < 0.5$. Limits of $\mu_{\tau\tau}$ is given in units of Bohr magneton and Λ is taken to be 1 GeV for limits of α_1^2 and α_2^2.

Luminosity:	10 fb^{-1}	30 fb^{-1}	50 fb^{-1}	100 fb^{-1}	200 fb^{-1}
$\mu_{\tau\tau}$	4.55×10^{-6}	3.79×10^{-6}	3.47×10^{-6}	3.06×10^{-6}	2.68×10^{-6}
α_1^2	2.10×10^{-17}	1.21×10^{-17}	9.37×10^{-18}	6.63×10^{-18}	4.69×10^{-18}
α_2^2	2.10×10^{-17}	1.21×10^{-17}	9.37×10^{-18}	6.63×10^{-18}	4.69×10^{-18}

TABLE II.   The same as Table I but for $0.0015 < \xi < 0.15$.

Luminosity:	10 fb^{-1}	30 fb^{-1}	50 fb^{-1}	100 fb^{-1}	200 fb^{-1}
$\mu_{\tau\tau}$	5.08×10^{-6}	4.23×10^{-6}	3.87×10^{-6}	3.41×10^{-6}	2.99×10^{-6}
α_1^2	7.16×10^{-17}	4.13×10^{-17}	3.20×10^{-17}	2.27×10^{-17}	1.60×10^{-17}
α_2^2	7.16×10^{-17}	4.13×10^{-17}	3.20×10^{-17}	2.27×10^{-17}	1.60×10^{-17}

TABLE III.   The same as Table I but for $0.1 < \xi < 0.5$.

Luminosity:	10 fb^{-1}	30 fb^{-1}	50 fb^{-1}	100 fb^{-1}	200 fb^{-1}
$\mu_{\tau\tau}$	3.40×10^{-6}	2.82×10^{-6}	2.58×10^{-6}	2.27×10^{-6}	1.98×10^{-6}
α_1^2	4.10×10^{-18}	2.37×10^{-18}	1.84×10^{-18}	1.30×10^{-18}	9.17×10^{-19}
α_2^2	4.10×10^{-18}	2.37×10^{-18}	1.84×10^{-18}	1.30×10^{-18}	9.17×10^{-19}

originates from the fact that although the cross sections in $0.1 < \xi < 0.5$ case are small, deviations of the anomalous cross sections from the standard model value are considerably large compare to $0.0015 < \xi < 0.15$ and $0.0015 < \xi < 0.5$ cases.

IV. CONCLUSIONS

Forward physics program of ATLAS and CMS collaborations provides an enhancement of the physics studied at the LHC. It allows us to study photon-photon and photon-proton interactions at energies higher than at any existing collider. LHC as a photon-photon or photon-proton collider presents an ideal venue to probe neutrino electromagnetic properties at a high energy.

We have investigated the potential of $pp \to p\gamma p \to p\nu\bar{\nu}qX$ reaction at the LHC to probe neutrino-photon and neutrino-two photon couplings. We show that this reaction has a great potential to probe neutrino-two photon couplings. It improves the sensitivity limits by up to a factor of 10^9 with respect to LEP limits. Our limits are also better than the limits obtained in reactions $pp \to p\gamma\gamma p \to p\nu\bar{\nu}p$ and $pp \to p\gamma\gamma p \to p\nu\bar{\nu}Zp$ at the LHC [43]. On the other hand, our limits on neutrino-photon coupling $\mu_{\tau\tau}$ are approximately an order of magnitude worse than the current experimental bound.

APPENDIX: ANALYTICAL EXPRESSIONS FOR G_1 AND G_2

In the case of effective interaction $\nu\bar{\nu}\gamma\gamma$ the polarization summed amplitude square for the subprocess $\gamma q \to \nu_i \bar{\nu}_j q$ ($q = u, d, c, s, b$) is given by

$$\langle |M_1|^2 \rangle = -\frac{16 Q^2 g_e^2}{q_1^4} \left[\frac{|\alpha_{R1}^{ij}|^2 + |\alpha_{L1}^{ij}|^2 + |\alpha_{R2}^{ij}|^2 + |\alpha_{L2}^{ij}|^2}{\Lambda^6} \right] \{ 2m_q^2((p_1 \cdot p_2)^2 - p_1 \cdot p_5 p_1 \cdot p_2 + (p_1 \cdot p_5)^2)$$
$$- ((p_1 \cdot p_2)^2 + (p_1 \cdot p_5)^2) p_2 \cdot p_5 \} p_3 \cdot p_4 \tag{A1}$$

$$\langle M_1^\dagger M_2 + M_2^\dagger M_1 \rangle = 0, \qquad \langle M_1^\dagger M_3 + M_3^\dagger M_1 \rangle = 0 \tag{A2}$$

$$\langle |M_2|^2 \rangle = \frac{4 g_Z^4 Q^2 g_e^2}{(q_2^2 - m_q^2)^2 (q_3^2 - m_Z^2)^2} \{ -(c_A^q - c_V^q)^2 p_4 \cdot p_5 (m_q^2 p_2 \cdot p_3 + p_1 \cdot p_3(m_q^2 - p_1 \cdot p_2))$$
$$- m_q^2(c_A^{q2} - c_V^{q2})(m_q^2 + p_1 \cdot p_2) p_3 \cdot p_4 - (c_A^q + c_V^q)^2 p_3 \cdot p_5 (m_q^2 p_2 \cdot p_4 + (m_q^2 - p_1 \cdot p_2) p_1 \cdot p_4) \} \delta_{ij} \tag{A3}$$

$$\langle |M_3|^2 \rangle = \frac{4 g_Z^4 Q^2 g_e^2}{(q_4^2 - m_q^2)^2 (q_3^2 - m_Z^2)^2} \{ (c_A^q - c_V^q)^2 (m_q^2 + p_1 \cdot p_5) p_1 \cdot p_4 p_2 \cdot p_3 + (c_A^q + c_V^q)^2 (m_q^2 + p_1 \cdot p_5) \times p_1 \cdot p_3 p_2 \cdot p_4$$
$$- m_q^2((c_A^q - c_V^q)^2 p_2 \cdot p_3 p_4 \cdot p_5 + (c_A^q + c_V^q)((c_A^q - c_V^q)(m_q^2 - p_1 \cdot p_5) p_3 \cdot p_4 + (c_A^q + c_V^q) p_2 \cdot p_4 p_3 \cdot p_5)) \} \delta_{ij} \tag{A4}$$

$$\langle M_2^\dagger M_3 + M_3^\dagger M_2 \rangle = \frac{4 g_Z^4 Q^2 g_e^2}{(q_2^2 - m_q^2)(q_4^2 - m_q^2)(q_3^2 - m_Z^2)^2} \{ (c_A^q)^2 p_1 \cdot p_4 p_2 \cdot p_3 p_2 \cdot p_5 + m_q^2(c_A^q)^2 p_1 \cdot p_2 p_3 \cdot p_4$$
$$- 2m_q^2(c_A^q)^2 p_2 \cdot p_5 p_3 \cdot p_4 + (c_A^q)^2 p_1 \cdot p_2 p_2 \cdot p_4 p_3 \cdot p_5 - 2(c_A^q)^2 p_2 \cdot p_4 p_2 \cdot p_5 p_3 \cdot p_5$$
$$- 2c_V^q c_A^q p_1 \cdot p_4 p_2 \cdot p_3 p_2 \cdot p_5 + 2c_V^q c_A^q p_1 \cdot p_2 p_2 \cdot p_4 p_3 \cdot p_5 - 2c_V^q c_A^q p_1 \cdot p_4 p_2 \cdot p_5 p_3 \cdot p_5$$
$$- 4c_V^q c_A^q p_2 \cdot p_4 p_2 \cdot p_5 p_3 \cdot p_5 + (c_V^q)^2 p_1 \cdot p_4 p_2 \cdot p_3 p_2 \cdot p_5 - (c_V^q)^2 m_q^2 p_1 \cdot p_2 p_2 \cdot p_3 p_4$$
$$+ 2(c_V^q)^2 m_q^2 p_2 \cdot p_5 p_3 \cdot p_4 + (c_V^q)^2 p_1 \cdot p_2 p_2 \cdot p_4 p_3 \cdot p_5 - (c_V^q)^2 p_1 \cdot p_4 p_2 \cdot p_5 p_3 \cdot p_5$$
$$- 2(c_V^q)^2 p_2 \cdot p_4 p_2 \cdot p_5 p_3 \cdot p_5 + (p_2 \cdot p_3(p_1 \cdot p_2 - 2p_2 \cdot p_5)(c_A^q - c_V^q)^2 + 2(c_A^{q2} + c_V^{q2}) p_1 \cdot p_2 p_3 \cdot p_5)$$
$$\times p_4 \cdot p_5 + p_1 \cdot p_3(p_2 \cdot p_5((c_A^q + c_V^q)^2 p_2 \cdot p_4 - (c_A^q - c_V^q)^2 p_4 \cdot p_5) - 2m_q^2(c_A^{q2} - c_V^{q2}) p_1 \cdot p_4)$$
$$+ p_1 \cdot p_5((c_A^q + c_V^q)(-(c_A^q - c_V^q) m_q^2 p_3 \cdot p_4 - (c_A^q + c_V^q) p_2 \cdot p_4 p_3 \cdot p_5) + p_2 \cdot p_3(-p_4 \cdot p_5(c_A^q - c_V^q)^2$$
$$- 2(c_A^{q2} + c_V^{q2}) p_2 \cdot p_4)) - (c_A^q)^2 p_1 \cdot p_4 p_2 \cdot p_5 p_3 p_3 \cdot p_5 \} \delta_{ij} \tag{A5}$$

$$g_Z = \frac{g_e}{\sin\theta_W \cos\theta_W}, \quad g_e = \sqrt{4\pi\alpha}, \quad Q = \tfrac{2}{3}, \quad c_A^q = \tfrac{1}{2}, \quad c_V^q = \tfrac{1}{2} - \tfrac{4}{3}\sin^2\theta_W \quad (q = u, c, t)$$
$$Q = -\tfrac{1}{3}, \quad c_A^q = -\tfrac{1}{2}, \quad c_V^q = -\tfrac{1}{2} + \tfrac{2}{3}\sin^2\theta_W \quad (q = d, s, b), \tag{A6}$$

where M_1, M_2 and M_3 are the amplitudes of the Feynman diagrams in Fig. 3. p_1 and p_2 are the momenta of incoming photon and quark and p_3, p_4 and p_5 are the momenta of outgoing neutrino, antineutrino and quark, respectively. Propagator momenta are defined by $q_1 = p_2 - p_5$, $q_2 = p_1 + p_2$, $q_3 = p_3 + p_4$, $q_4 = p_5 - p_1$. Therefore G_1 and G_2 functions in Eq. (6) are defined through the following equations:

$$(\alpha_1^2 + \alpha_2^2)G_1 = \sum_{i,j} \langle |M_1|^2 \rangle \tag{A7}$$

$$G_2 = 3\langle |M_2 + M_3|^2 \rangle. \tag{A8}$$

In the case of antiquarks (subprocess $\gamma\bar{q} \to \nu_i\bar{\nu}_j\bar{q}$) SM amplitudes (A3)–(A5) are modified but nonstandard contributions (A1) and (A2) remain unchanged.

---

[1] B. W. Lee and R. E. Schrock, Phys. Rev. D **16,** 1444 (1977).

[2] W. Marciano and A. I. Sanda, Phys. Lett. B **67,** 303 (1977).

[3] B. W. Lynn, Phys. Rev. D **23,** 2151 (1981).

[4] R. J. Crewther, J. Finjord, and P. Minkowski, Nucl. Phys. **B207,** 269 (1982).

[5] S. Dodelson and G. Feinberg, Phys. Rev. D **43,** 913 (1991).

[6] C. Royon *et al.* (RP220 Collaboration), arXiv:0706.1796 [physics.ins-det], *Proceedings for the DIS 2007 Workshop, Munich, 2007.*

[7] M. G. Albrow *et al.* (FP420 R and D Collaboration), JINST **4,** T10001 (2009).

[8] V. Avati and K. Osterberg, Report No. CERN-TOTEM-NOTE-2005-002, 2006.

[9] C. Royon, Mod. Phys. Lett. A **18,** 2169 (2003).

[10] M. Boonekamp, R. Peschanski, and C. Royon, Phys. Rev. Lett. **87,** 251806 (2001).

[11] M. Boonekamp, R. Peschanski, and C. Royon, Nucl. Phys. **B669,** 277 (2003).

[12] M. Boonekamp, A. De Roeck, R. Peschanski, and C. Royon, Phys. Lett. B **550,** 93 (2002).

[13] V. A. Khoze, A. D. Martin, and M. G. Ryskin, Eur. Phys. J. C **19,** 477 (2001).

[14] V. A. Khoze, A. D. Martin, and M. G. Ryskin, Eur. Phys. J. C **24,** 581 (2002).

[15] V. A. Khoze, A. D. Martin, and M. G. Ryskin, Eur. Phys. J. C **55,** 363 (2008).

[16] V. A. Khoze, A. D. Martin, and M. G. Ryskin, Phys. Lett. B **650,** 41 (2007).

[17] A. B. Kaidalov, V. A. Khoze, A. D. Martin, and M. G. Ryskin, Eur. Phys. J. C **33,** 261 (2004).

[18] A. B. Kaidalov, V. A. Khoze, A. D. Martin, and M. G. Ryskin, Eur. Phys. J. C **31,** 387 (2003).

[19] O. Kepka and C. Royon, Phys. Rev. D **78,** 073005 (2008).

[20] V. A. Khoze, A. D. Martin, and M. G. Ryskin, Eur. Phys. J. C **23,** 311 (2002).

[21] N. Schul and K. Piotrzkowski, Nucl. Phys. B, Proc. Suppl. **179–180,** 289 (2008).

[22] S. R. Klein and J. Nystrand, Phys. Rev. Lett. **92,** 142003 (2004).

[23] M. B. Gay Ducati and G. G. Silveira, Phys. Rev. D **82,** 073004 (2010).

[24] V. P. Goncalves and M. V. T. Machado, Phys. Rev. D **75,** 031502 (2007).

[25] M. V. T. Machado, Phys. Rev. D **78,** 034016 (2008)

[26] K. Piotrzkowski, Phys. Rev. D **63,** 071502 (2001).

[27] X. Rouby, Ph.D. thesis, Universite catholique de Louvain [UCL-Thesis 135-2008, CMS TS-2009/004], 2008.

[28] A. Abulencia *et al.* (CDF Collaboration), Phys. Rev. Lett. **98,** 112001 (2007).

[29] T. Aaltonen *et al.* (CDF Collaboration), Phys. Rev. Lett. **99,** 242002 (2007).

[30] T. Aaltonen *et al.* (CDF Collaboration), Phys. Rev. Lett. **102,** 242001 (2009).

[31] T. Aaltonen *et al.* (CDF Collaboration), Phys. Rev. Lett. **102,** 222002 (2009).

[32] V. M. Budnev, I. F. Ginzburg, G. V. Meledin, and V. G. Serbo, Phys. Rep. **15,** 181 (1975).

[33] G. Baur *et al.*, Phys. Rep. **364,** 359 (2002).

[34] S. M. Lietti, A. A. Natale, C. G. Roldao, and R. Rosenfeld, Phys. Lett. B **497,** 243 (2001).

[35] E. Chapon, C. Royon, and O. Kepka, Phys. Rev. D **81,** 074003 (2010).

[36] S. Atağ, S. C. İnan, and İ. Şahin, Phys. Rev. D **80,** 075009 (2009).

[37] İ. Şahin and S. C. İnan, J. High Energy Phys. 09 (2009) 069.

[38] S. Atağ, S. C. İnan, and İ. Şahin, J. High Energy Phys. 09 (2010) 042.

[39] S. C. İnan, Phys. Rev. D **81,** 115002 (2010).

[40] S. Atağ and A. A. Billur, J. High Energy Phys. 11 (2010) 060.

[41] M. G. Albrow, T. D. Coughlin, and J. R. Forshaw, Prog. Part. Nucl. Phys. **65,** 149 (2010).

[42] İ. Şahin, and A. A. Billur, Phys. Rev. D **83,** 035011 (2011).

[43] İ. Şahin and M. Koksal, J. High Energy Phys. 03 (2011) 100.

[44] F. Larios, R. Martinez, and M. A. Perez, Phys. Lett. B **345**, 259 (1995).

[45] M. Maya, M. A. Perez, G. Tavares-Velasco, and B. Vega, Phys. Lett. B **434**, 354 (1998).

[46] N. F. Bell, V. Cirigliano, M. J. Ramsey-Musolf, P. Vogel, and M. B. Wise, Phys. Rev. Lett. **95**, 151802 (2005).

[47] F. Larios, M. A. Perez, and G. Tavares-Velasco, Phys. Lett. B **531**, 231 (2002).

[48] J. F. Nieves, Phys. Rev. D **28**, 1664 (1983).

[49] R. K. Ghosh, Phys. Rev. D **29**, 493 (1984).

[50] J. Liu, Phys. Rev. D **44**, 2879 (1991).

[51] S. N. Gninenko and N. V. Krasnikov, Phys. Lett. B **450**, 165 (1999).

[52] H. B. Li et al. (TEXONO Collaboration), Phys. Rev. Lett. **90**, 131802 (2003).

[53] Z. Daraktchieva et al. (MUNU collaboration), Phys. Lett. B **615**, 153 (2005).

[54] H. T. Wong et al. (TEXONO Collaboration), Phys. Rev. D **75**, 012001 (2007).

[55] H. T. Wong, H.-B. Li, and S.-T. Lin, Phys. Rev. Lett. **105**, 061801 (2010).

[56] C. Arpesella et al. (The Borexino collaboration), Phys. Rev. Lett. **101**, 091302 (2008).

[57] G. G. Raffelt, Phys. Rep. **320**, 319 (1999).

[58] V. Castellani and S. Degl'Innocenti, Astrophys. J. **402**, 574 (1993).

[59] M. Catelan, J. A. dPacheco, and J. E. Horvath, Astrophys. J. **461**, 231 (1996).

[60] A. Ayala, J. C. D'Olivo, and M. Torres, Phys. Rev. D **59**, 111901 (1999).

[61] R. Barbieri and R. N. Mohapatra, Phys. Rev. Lett. **61**, 27 (1988).

[62] J. M. Lattimer and J. Cooperstein, Phys. Rev. Lett. **61**, 23 (1988).

[63] A. Heger, A. Friedland, M. Giannotti, and V. Cirigliano, Astrophys. J. **696**, 608 (2009).

[64] A. D. Martin, W. J. Stirling, R. S. Thorne, and G. Watt, Phys. Lett. B **652**, 292 (2007).

[65] R. Schwienhorst et al. (DONUT Collaboration), Phys. Lett. B **513**, 23 (2001).

[66] S. Davidson, M. Gorbahn, and A. Santamaria, Phys. Lett. B **626**, 151 (2005).